

# Throttleless premixed-charge engines: concept and experiment

P D Ronney, BS, MS, ScD, MemASME, MAIAA

Department of Mechanical Engineering, University of Southern California, Los Angeles, California, USA

M Shoda,\* BS, S T Waida, BSE and E J Durbin, BS, MS

Department of Mechanical and Aerospace Engineering, Princeton University, Princeton, New Jersey, USA

*A method of controlling the brake mean effective pressure (b.m.e.p.) of a premixed-charge engine is proposed which does not require the use of a throttle and does not exhibit significant throttling losses. In this method, a combination of adjustment of the mixture equivalence ratio and preheating of the mixture is used to control the b.m.e.p. The preheating serves two purposes: it reduces the density of the mixture and it broadens the lean misfire limit. Experiments on the performance of engines controlled with this strategy are compared with conventional throttled engines. As much as 16 per cent improvement in thermal efficiency was observed at the same b.m.e.p. The untreated  $NO_x$  emissions are found to be much lower in the throttleless engine at the same b.m.e.p. while carbon monoxide (CO) and unburned hydrocarbon (UHC) emissions are comparable to but somewhat higher than throttled engines. Practical implementation of the concept is discussed.*

## NOTATION

b.m.e.p.	brake mean effective pressure
DACS	data acquisition and control system
EGR	exhaust gas recirculation
f.m.e.p.	friction mean effective pressure (rubbing only)
i.m.e.p.	indicated mean effective pressure (gross)
LML	lean misfire limit
MON	motor octane number
MBT	maximum brake torque
$N$	engine rotation rate
NG	natural gas
$NO_x$	nitrogen oxide emission
$\dot{m}_a$	mass flowrate of air into engine
$\dot{m}_f$	mass flowrate of fuel into engine
p.m.e.p.	pumping mean effective pressure
$P_{ex}$	exhaust pressure
$P_{in}$	intake manifold pressure
$r$	compression ratio
$R$	ideal gas constant
RON	research octane number
$T_{ad}$	constant-pressure adiabatic flame temperature
$T_{amb}$	ambient temperature
$T_{cyl}$	mean in-cylinder gas temperature at time of intake valve closing
$T_{eg}$	end-gas temperature
$T_{in}$	intake manifold gas temperature
TPCE	throttleless premixed-charge engine
UHC	unburned hydrocarbon
$V_d$	displacement volume
WOT	wide-open throttle
$\gamma$	gas specific heat ratio
$\Delta T_c$	temperature rise due to constant-volume combustion at $\phi = 1$
$\eta_{th}$	brake thermal efficiency
$\rho_{cyl}$	intake mixture density at $T_{cyl}$ and $P_{in}$
$\phi$	fuel-air equivalence ratio

## 1 INTRODUCTION

In most powerplant applications, particularly in vehicles, some means of adjusting the work output or brake mean effective pressure (b.m.e.p.) of the engine is required. In conventional premixed-charge (that is gasoline-fuelled, spark-ignition) engines,  $\phi$  is maintained at values close to unity and a throttle is used to adjust the value of  $\rho_{cyl}$ . This change in  $\rho_{cyl}$  changes the b.m.e.p., since b.m.e.p. is roughly proportional to the quantity of fuel burned in the cylinder(s). The throttle adjusts  $\rho_{cyl}$  by varying  $P_{in}$  via a pressure drop across a flow constriction. A significant problem with throttling is that work must be done in order to draw the sub-atmospheric mixture into the cylinder(s). Because this so-called 'throttling loss' results from an irreversible expansion across the throttle plate, it cannot be recovered elsewhere in the cycle (unlike, for example, compression work which ideally is recovered in the expansion stroke). Appendix 1 gives an estimate of the reduction in  $\eta_{th}$  due to throttling for a representative engine. Figure 1 shows that at light loads this loss may represent a very substantial portion of the otherwise available shaft work.

Non-premixed-charge (that is diesel-type) engines use a different strategy to adjust b.m.e.p. which does not lead to throttling losses.  $P_{in}$  is maintained at atmospheric pressure but the overall  $\phi$  (and thus the quantity of fuel burned in the cylinder(s)) is adjusted by controlling the amount of fuel injected into the cylinder(s) after compression. Such a technique is not applicable to premixed-charge engines because, when  $\phi$  is less than typically 0.7, a lean misfire condition occurs. This is not problematic in diesel-type engines because combustion occurs primarily in a non-premixed mode where chemical reaction takes place at near-stoichiometric surfaces between pure fuel and pure air. One major drawback of non-premixed combustion in engines is that finite fuel-air mixing times make it difficult to operate at near-stoichiometric conditions without unacceptable degradation of  $\eta_{th}$  and smoke emission. Consequently,

*This MS was received on 15 February 1993 and was accepted for publication on 21 June 1993.*

\* Present address: Komatsu Limited, Tochigi, Japan.

diesel-type engines generally have lower maximum b.m.e.p. than premixed-charge engines. Also, the near-stoichiometric burning surfaces and the resulting high flame temperatures lead to relatively high  $\text{NO}_x$  emissions, even at low overall  $\phi$  (1).

A concept (2) for controlling b.m.e.p. in a premixed-charge engine has been proposed in a manner that has some of the advantages of both premixed- and non-premixed-charge engines. In this concept, called the throttleless premixed-charge engine (TPCE), both  $\phi$  and  $\rho_{\text{cyl}}$  are adjusted, but  $\rho_{\text{cyl}}$  is adjusted by varying  $T_{\text{in}}$  rather than  $P_{\text{in}}$  (as with throttled engines). This is done by preheating the intake charge, which does not cause a significant pressure drop and thus does not cause a throttling loss. Preheating is employed only under conditions where the b.m.e.p. demand is less than the maximum available from the engine; at maximum b.m.e.p. demand the TPCE is identical to a conventional premixed-charge engine operating at wide-open throttle (WOT). In addition to decreasing  $\rho_{\text{cyl}}$ , preheating also reduces  $\phi$  at the lean misfire limit (LML) (3). This in turn extends the range of b.m.e.p. adjustment that is attainable through varying  $\phi$  in a premixed-charge engine. While preheating will promote knock, the knock-limited values of  $T_{\text{in}}$  are generally much higher for the lean mixtures which are employed in conjunction with higher  $T_{\text{in}}$  (4, 5).

The use of heat exchange between the combustible gases and their exhaust products in the present work owes its genesis to the studies by Weinberg and collaborators (6, 7). These authors found it was possible to burn mixtures much leaner than any conventional flammability limit, without any external energy input, by preheating the gases with thermal energy from their burned gases in a well-insulated counterflow heat exchanger.

A schematic diagram of the probable operating limits of a TPCE in the  $\phi$ - $T_{\text{in}}$  plane is shown in Fig. 1. Rich

mixtures ( $\phi > 1$ ) are excluded for reasons of fuel economy and emissions performance, and mixtures with  $T_{\text{in}} < T_{\text{amb}}$  are excluded because no means of cooling the charge is available. The minimum  $\phi$  is determined by the LML and the maximum is set by  $\phi = 1$  or the knock limit (see Appendix 2). The maximum reduction in b.m.e.p. occurs at the operating condition corresponding to the intersection of the knock and misfire limit curves. Lines of constant fuel input, and thus constant i.m.e.p. = b.m.e.p. + f.m.e.p. according to ideal-cycle analysis, are also shown (note that by assumption p.m.e.p. = 0). Within the limits shown in Fig. 1 the combination of  $\phi$  and  $T_{\text{in}}$  may be chosen for a given b.m.e.p. which optimizes a specified performance criterion, for example  $\eta_{\text{th}}$  or  $\text{NO}_x$  emissions.

The use of lean mixtures in the TPCE is expected to reduce untreated  $\text{NO}_x$  emissions compared to a conventional throttled engine but could lead to higher unburned hydrocarbon (UHC) and carbon monoxide (CO) emissions. However, the increased  $T_{\text{in}}$  could lead to higher flame temperatures and thus higher  $\text{NO}_x$  emissions. Hence, a characterization of the emissions performance of TPCEs is needed.

Another possible means to control the b.m.e.p. of a premixed-charge engine is by varying the amount of exhaust gas recirculation (EGR). An analysis (not shown) analogous to that in Appendix 2 indicates that the ideal performance of this scheme, in terms of the controllable b.m.e.p. range and improvement in  $\eta_{\text{th}}$  over throttled engines, is the same as with the TPCE concept. Hence, the possibility of control of b.m.e.p. via EGR also needs to be assessed.

## 2 OBJECTIVES AND APPROACH

The goal of this work is to explore the feasibility of the TPCE and EGR-controlled engines and to compare

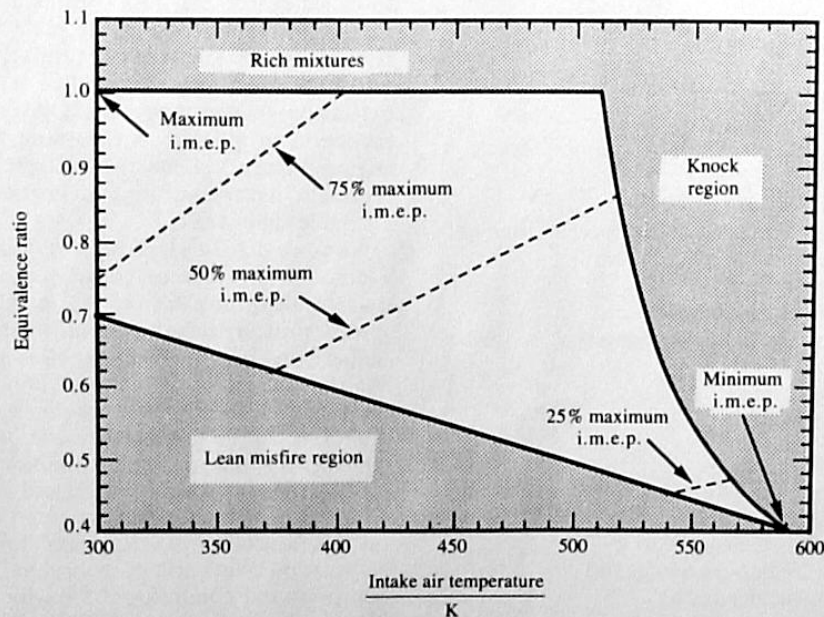


Fig. 1 Conjectured operating map of an NG (natural gas)-fuelled TPCE (see Appendix 2)

their performance to throttle-controlled engines. TPCE experiments were performed by maintaining WOT conditions and varying both  $\phi$  and  $T_{in}$  to adjust b.m.e.p. EGR experiments were performed by maintaining WOT conditions, holding  $T_{in} = T_{amb}$ , and varying both  $\phi$  and the amount of EGR to adjust b.m.e.p. Conventional throttling experiments were performed by operating at  $\phi = 1$ ,  $T_{in} = T_{amb}$  and varying throttle position (thus  $P_{in}$ ) to adjust b.m.e.p. Because some important operating characteristics, notably knock, are strongly affected by the type of fuel, two different fuels were employed: NG because of its excellent knock performance (RON  $\approx$  120, MON  $\approx$  120) and commercial unleaded gasoline (RON + MON)/2 = 89.

In each experiment  $T_{in}$ ,  $\dot{m}_a$ ,  $\dot{m}_f$ ,  $N$ , brake torque and exhaust emissions were measured. From this information  $\phi$ , b.m.e.p. and  $\eta_{th}$  were determined. The ignition timing was set to that providing maximum brake torque (MBT) except where this caused knocking, in which case the timing was retarded until the knocking just ceased. The presence or absence of knocking was determined audibly. The knock limit was defined as the limiting conditions (of  $\phi$  and  $T_{in}$ ) for which the spark timing could be advanced to MBT without knocking. The LML was defined as the lowest  $\phi$  (for a given  $T_{in}$ ) for which the engine would not exhibit audible misfire. The knock and misfire limit determinations, while subjective, were found to be well defined in that a small adjustment of spark timing or  $\phi$  would clearly move the engine into or out of knocking or misfiring conditions.

### 3 EXPERIMENTAL APPARATUS

The apparatus in which most of the experiments were conducted (Fig. 2) consisted of a production four-cylinder General Motors LX8 engine with  $V_d = 2.5$  litres and  $r = 8.2$  coupled to a water-brake dynamometer and a microcomputer-controlled data acquisition and control system (DACS). The factory intake and

exhaust manifolds were replaced with 11 litre plenums coupled to 4.5 cm diameter pipes which led to the appropriate ports in the cylinder head. This minimized the pressure fluctuations in the intake and exhaust system, which was considered important for a study of throttling effects. The intake air was heated by a set of electric resistance heater elements coupled to a microprocessor-based temperature regulator controlled by the DACS. In a practical TPCE, control of  $T_{in}$  would be accomplished by a heat exchanger between the intake and exhaust streams (see Section 5). The intake system was insulated to minimize heat losses. The stock ignition system was used with 1.5 mm gap spark plug.

The DACS consisted of a microcomputer and a multi-channel analogue-to-digital converter board. The DACS sensed the engine speed and adjusted the dynamometer load to maintain a constant, specified speed. Data were taken at two different  $N$  values (1200 and 2000 r/min), but since no significant differences were found only 1200 r/min results are reported here. At this speed the f.m.e.p. at WOT, as estimated by a Morse test, was about 0.68 bar and was nearly independent of  $T_{in}$ . The flowrate  $\dot{m}_a$  was measured by a turbine-type flowmeter. In the NG experiments, the fuel metering system consisted of a stepper-motor driven valve controlled by the DACS and a mass flowmeter monitored by the DACS. By measuring  $\dot{m}_a$  and  $\dot{m}_f$ ,  $\phi$  could be determined and the valve position adjusted to maintain a specified  $\phi$ . The NG contained 96.1 per cent  $CH_4$ , 1.74 per cent  $C_2H_6$ , 0.44 per cent  $C_3H_8$ , 0.44 per cent higher hydrocarbons, 0.90 per cent  $CO_2$  and 0.38 per cent  $N_2$ . In the liquid-fuel experiments, a production port fuel-injection system with variable  $\phi$  capability was employed and  $\dot{m}_f$  was measured by a positive-displacement flowmeter read by the DACS.

The EGR tests and emissions measurements were conducted at the SouthWest Research Institute (San Antonio, Texas) using a four-cylinder Ford LSG423 with  $V_d = 2.3$  litre and  $r = 8.0$ . The apparatus was very

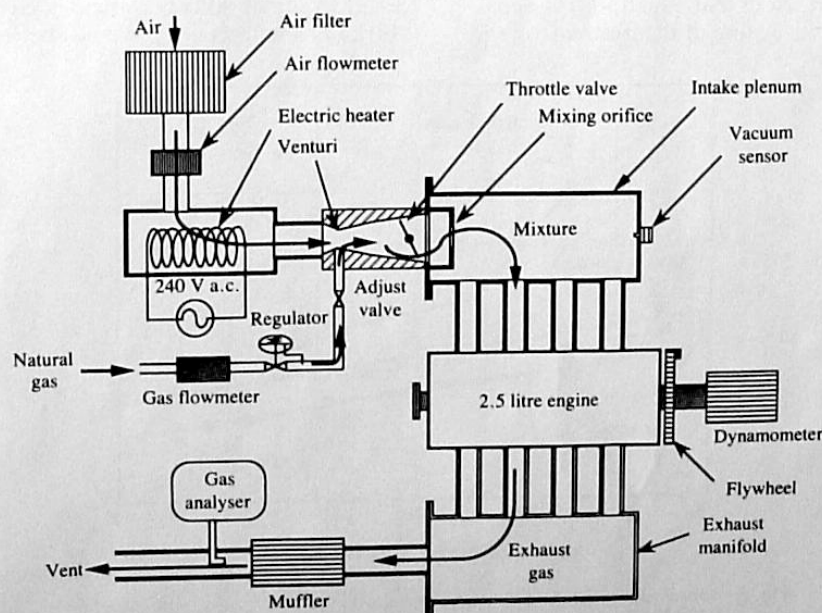


Fig. 2 Experimental apparatus block diagram (illustrated for NG fuel system)



similar to that described above. The comparisons of the performance of this engine in the throttled and TPCE modes were practically identical to those in the system described above and so are not presented in detail here. A gate valve was used to control the amount of exhaust gas fed back into the intake plenum of this engine. The intake, exhaust and EGR plumbing was insulated to minimize heat losses. Exhaust emissions were analysed for  $\text{NO}_x$ , CO and UHC using standard instrumentation.

For both engines,  $T_{in}$  was measured by thermocouples whose output voltages were read by the DACS. The thermocouple junctions were located as close as possible to the intake valves in order to minimize errors caused by heat losses in the intake manifold. However, from an examination of volumetric efficiency data at WOT, it was inferred that the mean gas temperature in the cylinders at intake valve closing ( $T_{cyl}$ ) was not the same as  $T_{in}$ . This was probably due to the heat transfer that occurred as the charge passed the intake valves and settled in the cylinders. In order to provide reliable initial conditions for misfire, emissions and knock modelling,  $T_{cyl}$  must be known accurately. Hence,  $T_{cyl}$  was inferred in the following way. First  $\rho_{cyl}$  can be estimated as  $2(\dot{m}_a + \dot{m}_f)/V_d N$ . Since all tests with heated intake charges were performed at  $P_{in} = 1$  atm and because the low engine speeds employed in this work ensured that pressure losses in the intake system were small, it can be assumed that the cylinder pressure at intake valve closing is nearly equal to  $P_{in}$ . Then  $T_{cyl}$  can be estimated as  $P_{in}/\rho_{cyl} R$ .  $T_{cyl}$  inferred in this way was found empirically (5) to be related to  $T_{in}$ , nearly independent of  $N$ , according to

$$T_{cyl} \approx T_{ref} + C(T_{in} - T_{ref}) \quad \text{for } C \approx 0.58 \quad (1)$$

where  $T_{ref} = 373$  K.  $T_{ref}$  can be interpreted as an average wall temperature during the intake process, which should be slightly higher than the cooling water temperature (and indeed 373 K satisfies this criterion).  $C^{-1} - 1$  can be interpreted as a dimensionless overall heat-transfer coefficient. Note that equation (1) approximately accounts for the heating of the fresh mixture by

the exhaust residual as well, because this heating will be reflected in a lower  $\dot{m}_a + \dot{m}_f$  and thus a lower calculated  $\rho_{cyl}$ .

Heat loss during compression was inferred to be small by comparing motored pressure traces (5) recorded for different  $T_{in}$  (not shown). If heat losses are small and  $\gamma$  is constant, then the peak pressure should be independent of  $T_{in}$ . A small decrease in peak pressure was observed at higher  $T_{in}$ , but this decrease is nearly that expected when the lower  $\gamma$  at higher temperatures is considered.

## 4 RESULTS

### 4.1 Operating map

Figure 3 shows the misfire and knock limits of TPCEs operating with NG and gasoline fuels. The value of  $\phi$  at the LML decreases almost linearly with increasing  $T_{in}$  and is similar for the two fuels. Similar behaviour is found in laboratory experiments of lean flammability limits (8). The knock-limited values of  $T_{in}$  at a given  $\phi$  are quite different for the two fuels, but in both cases are much higher for lower  $\phi$ , consistent with previous studies (4). Thus, there is a band of misfire-free, knock-free operating conditions up to relatively high  $T_{in}$  and low  $\phi$ , indicating that a large range of b.m.e.p. control may be obtained without throttling. Note that, for gasoline, the knock and misfire limit curves converge at  $\phi \approx 0.55$ ,  $T_{in} = 530$  K, but the point of convergence for NG could not be reached with the preheating system employed here.

The effect of  $T_{in}$  and fuel type on the LML might be explained in the following way. The laminar flame speed depends mostly on  $T_{ad}$  rather than the initial temperature (9). If the turbulence properties in the engine do not change substantially with varying  $T_{in}$ , the turbulent flame speed would depend mainly on  $T_{ad}$  and not  $T_{in}$ . Since a minimum turbulent flame speed is needed to avoid lean misfire [since the burning time must be less than about 80 crank angle degrees to avoid misfire (10)], a minimum  $T_{ad}$  would be required to avoid

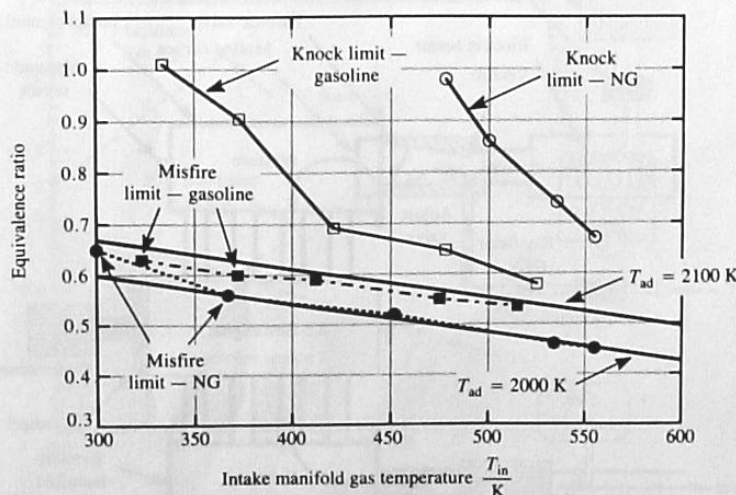


Fig. 3 Observed knock and flammability limits for NG- and gasoline-fuelled TPCE systems at 1200 r/min along with curves of computed  $T_{ad} = 2000$  and 2100 K



misfire. To test this hypothesis,  $T_{ad}$  was calculated as follows. The initial charge at  $T_{cyl}$  and  $P_{in}$  was first assumed to be compressed adiabatically (which was shown in Section 3 to be approximately valid) at frozen composition by a volume ratio of 8.2. This gas was then assumed to burn to equilibrium at constant pressure. While only the early stage of burning will be at nearly constant pressure, the delay in flame kernel development at this stage is largely responsible for the behaviour of the LML (11). The actual  $T_{ad}$  is estimated to be the calculated equilibrium temperature of the burned gas. A chemical equilibrium computer program was used to determine the state of the gas at the end of compression and combustion processes. Figure 3 shows that the LML corresponds to values of  $T_{ad}$ , calculated in this way, between 2000 and 2100 K for both fuels. This similarity between fuels is understandable since  $T_{ad}$  and thus the laminar flame speed is similar for many hydrocarbons at the same  $\phi$  and initial temperature (9).

The observed knock performance of lean mixtures is considerably better than the rough estimates shown in Fig. 1. The knock properties of lean mixtures seems to have received relatively little attention in the literature [reference (4) being an exception]. A recent study of these properties is presented elsewhere (5).

#### 4.2 Fuel efficiency

Figure 4 shows the effect of  $\phi$  and  $T_{in}$  on b.m.e.p. for the TPCE. For clarity, only NG results are shown. The results for gasoline were very similar except that because of the poorer knock performance of gasoline, the maximum  $T_{in}$  attainable without knock is lower. For each  $T_{in}$ , b.m.e.p. decreases as  $\phi$  decreases. At first the decrease is almost linear, which is expected since the heat input is nearly linear with  $\phi$  (see Appendix 1). As  $\phi$  decreases further, the decrease becomes steeper, indicating the approach to the LML. At higher  $T_{in}$ , the maximum b.m.e.p. is lower because  $\rho_{cyl}$  is lower and the value of  $\phi$  where the curves begin to steepen is lower. The outer envelope of these points represents combinations of  $\phi$  and  $T_{in}$  which provide the best  $\eta_{th}$  for a

given b.m.e.p. These points, examples of which are identified by the arrows in Fig. 4, will be denoted 'best TPCE' in later discussion. All other points will be denoted 'other TPCE'.

Figure 5 shows a comparison of  $\dot{m}_f$  for the TPCE and throttled engine plotted against b.m.e.p. Again, only NG results are shown. The results are presented in this way because it shows the improvement in fuel consumption for a given b.m.e.p. which is possible with the TPCE. The dotted line shows the sum of the b.m.e.p. and manifold vacuum for each operating point for the throttled engine. This line provides an estimate of the b.m.e.p. that the throttled engine would provide if there were no pumping loss. The fact that this line falls on top of much of the TPCE data (except at the highest b.m.e.p.) shows that most of the improvement of the TPCE over the throttled engine is due to the elimination of throttling losses.

Figure 6 shows the improvement in  $\eta_{th}$  of NG- and gasoline-fuelled TPCEs over their throttled counterparts as a function of b.m.e.p./b.m.e.p.<sub>WOT</sub>. The improvement is similar for both fuels and increases as b.m.e.p. decreases because of the greater throttling loss at lower b.m.e.p. The maximum observed improvement, about 16 per cent at 27 per cent of the maximum b.m.e.p., is greater for NG because it is possible to obtain lower b.m.e.p. in this case. This in turn is because of the better knock performance of NG, which allows higher values of  $T_{in}$  and thus lower b.m.e.p. to be obtained. At higher b.m.e.p., the experimental data show slightly greater improvement in  $\eta_{th}$  than the estimates given in Appendix 1. This suggests that a small portion of the improvement in  $\eta_{th}$  occurs for a reason other than the elimination of throttling losses, for example more complete burning of the fuel for lean mixtures. Also, for low b.m.e.p., the improvement is less than predicted because at these conditions high values of  $T_{in}$  are employed and in many cases, especially for the gasoline, the spark timing must be retarded from MBT to avoid knock.

A comparison of  $\eta_{th}$  (referenced to its value at WOT) for throttled, TPCE and EGR-controlled NG-fuelled

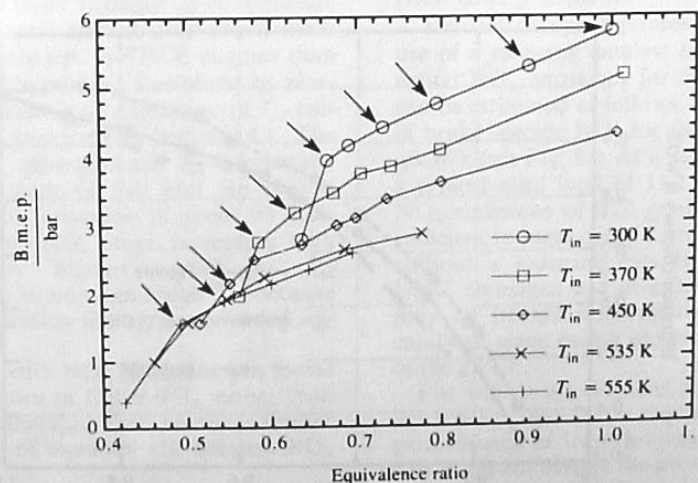
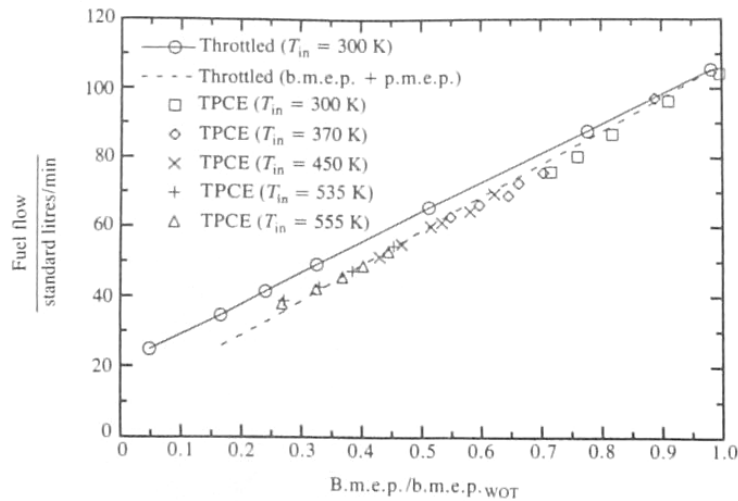
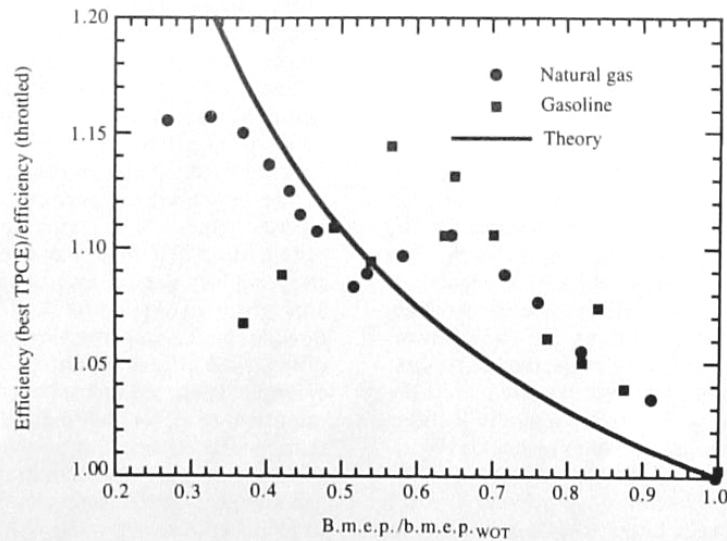


Fig. 4 Observed b.m.e.p. of an NG-fuelled TPCE engine at 1200 r/min as a function of  $\phi$  for several values of  $T_{in}$ . Arrows are described in the text



**Fig. 5** Observed fuel flow for NG-fueled throttled and throttleless engines at 1200 r/min as a function of b.m.e.p. Dashed line is the sum of the throttled engine b.m.e.p. and manifold vacuum



**Fig. 6** Measured ratio of brake thermal efficiencies of throttled and throttleless engines for NG- and gasoline-fueled engines at 1200 r/min and comparison with the predictions of equation (11)

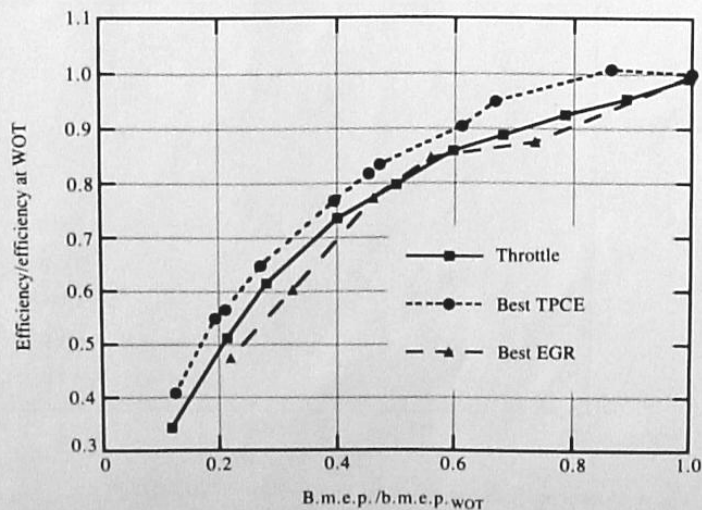


**Fig. 7** Comparison of brake thermal efficiency, referenced to the value at WOT, for throttle-, TPCE- and EGR-controlled NG-fueled engines at 1200 r/min as a function of b.m.e.p./b.m.e.p.WOT

engines is shown in Fig. 7;  $\eta_{th}$  for throttled and EGR-controlled engines is inferior to that of TPCE engines. The inferior performance of throttled engines has already been discussed. The inferior performance of EGR control probably occurs for the same reason that it works well as an  $NO_x$  control mechanism, namely the reduction in  $T_{ad}$  due to dilution of the combustible mixture by the exhaust gases. The reduction in  $T_{ad}$  leads to a reduction in the turbulent flame speed and an increase in the value of  $\phi$  at the LML for the reasons described in Section 4.1. Thus, the use of EGR to reduce b.m.e.p. results in a lowering of  $T_{ad}$ , which is unlike the TPCE in that preheating raises  $T_{ad}$ . Consequently, EGR control does not provide an improvement in  $\eta_{th}$  over throttled engines, nor as much range of b.m.e.p. control as the TPCE\* (although no knock limitations were observed with EGR). Hence, there is little apparent value for using EGR control as an alternative to the TPCE concept.

### 4.3 Emissions performance

Figure 8a shows that the untreated brake specific (BS)  $NO_x$  levels of the 'best TPCE' points were more than an order of magnitude lower than the throttled engine at the same b.m.e.p. Hence, both substantially improved fuel economy and substantially reduced  $NO_x$  emissions compared to throttled engines may be obtained simultaneously with the TPCE. It should be noted that no attempt was made to reduce  $NO_x$  by retarding the timing slightly from MBT; thus,  $NO_x$  levels somewhat lower than those shown in Fig. 8a may be attainable without significant degradation in  $\eta_{th}$ . Figure 8a also shows that the use of EGR is somewhat better than TPCE for reducing  $NO_x$  emissions in many cases (but at the expense of substantially lower  $\eta_{th}$ , as discussed in Section 4.2).

The improvement in  $NO_x$  emissions with the TPCE as compared to the throttled engine is probably due to the lower values of  $T_{ad}$  characteristic of many of the TPCE points. This is because  $T_{ad}$  decreases much more rapidly with decreasing  $\phi$  (as in the TPCE) than with decreasing  $P_{in}$  (as in a throttled engine). Since thermal  $NO_x$  levels depend much more strongly on temperature than pressure (1),  $NO_x$  levels should drop much more rapidly with decreasing b.m.e.p. in TPCE engines than in throttled engines. This hypothesis was tested by plotting (see Fig. 9)  $NO_x$  emissions as a function of  $T_{ad}$  calculated by the method described in Section 4.1. The correlation between  $NO_x$  emissions and  $T_{ad}$  is generally quite good. (From the slope of this plot, an overall activation energy for  $NO_x$  formation of about 95 kcal/mol can be inferred.) The  $NO_x$  stops increasing with increasing  $T_{ad}$  at the highest values of  $T_{ad}$  (corresponding to  $\phi$  close to unity and high  $T_{in}$ ) because at these conditions the ignition timing was retarded significantly to avoid knock.

The correlation of  $T_{ad}$  with  $NO_x$  emissions was found to be inferior to that shown in Fig. 9 if  $T_{in}$  rather than  $T_{cy1}$  was used to estimate  $T_{ad}$ . This provides further support for the validity of equation (1), because  $NO_x$

formation is very sensitive to temperature and thus significant errors in the temperature correction proposed in equation (1) would lead to a poor correlation of  $NO_x$  emission with the calculated  $T_{ad}$ .

The CO emissions were slightly higher for the 'best TPCE' than the throttled engine at the same b.m.e.p. (Fig. 8b). The UHC emissions were also higher, particularly at low b.m.e.p. (Fig. 8c). These higher emissions are probably due to some incomplete burning, which inevitably occurs near the LML, even before the degree of incompleteness is sufficient to cause a noticeable reduction in  $\eta_{th}$ . The consequences of these higher UHC emissions is discussed in the following section.

## 5 PRACTICAL PERSPECTIVE

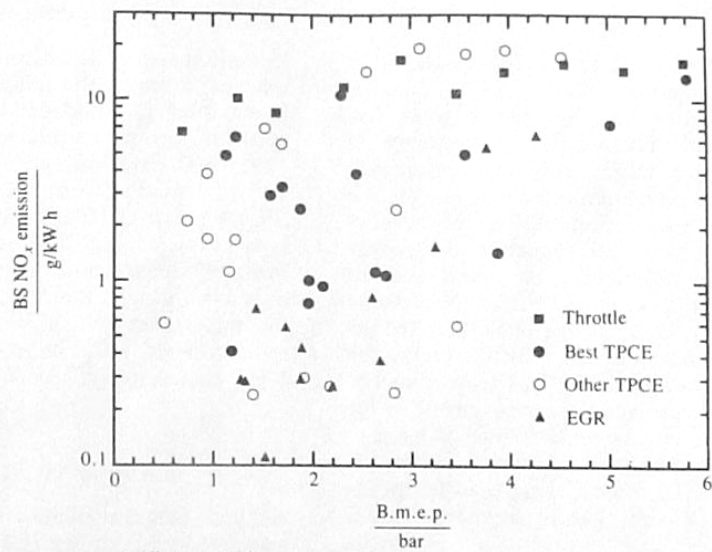
A block diagram of how the TPCE concept might be implemented is shown in Fig. 10. Other possible implementations are described elsewhere (2). The intake manifold is branched into preheated and non-preheated sections. The preheated section obtains thermal energy from the exhaust gases through a heat exchanger. The amount of preheat is controlled by a diverter valve in the intake manifold. The heated air is mixed with fuel and fed into the combustion chamber(s). Alternatively, port fuel injection may be employed. The ratio  $\phi$  and the level of preheating employed depend on the b.m.e.p. demand. Since many combinations of  $\phi$  and  $T_{in}$  will provide the same b.m.e.p. (see Fig. 1), there is flexibility to optimize performance depending upon the application. For most applications low  $NO_x$  emissions are required, but the improvements in  $\eta_{th}$  which are possible with the TPCE must not be compromised substantially. The results of Section 4 indicate that for these criteria the optimal operating condition is to use the leanest mixture which does not produce significant misfire and the corresponding reduction in  $\eta_{th}$ . If the b.m.e.p. is too large at this condition, greater preheat is employed and  $\phi$  is reduced to the new LML. Current industrial practice of using microprocessor-based controls on automotive engines would enable the TPCE to operate under the most favourable conditions for a given b.m.e.p. demand.

The use of lean mixtures in the TPCE preclude the use of a reducing catalyst to treat  $NO_x$  emissions. The actual  $NO_x$  emissions for a typical vehicle application can be estimated as follows. The readily attainable value of brake specific  $NO_x$  for the TPCE is not more than 1 g/kW h (see Fig. 8a). At a vehicle speed of 55 mile/h and a typical road load of 11.2 kW (15 h.p.) at 55 mile/h,  $NO_x$  emissions of 0.20 g/mile can be expected. This is sufficient to meet many current and proposed standards without a reducing catalyst. The untreated CO and UHC emissions are in excess of many standards but may be treated with relatively inexpensive oxidizing catalysts, since excess oxygen is present in the exhaust of the TPCE.

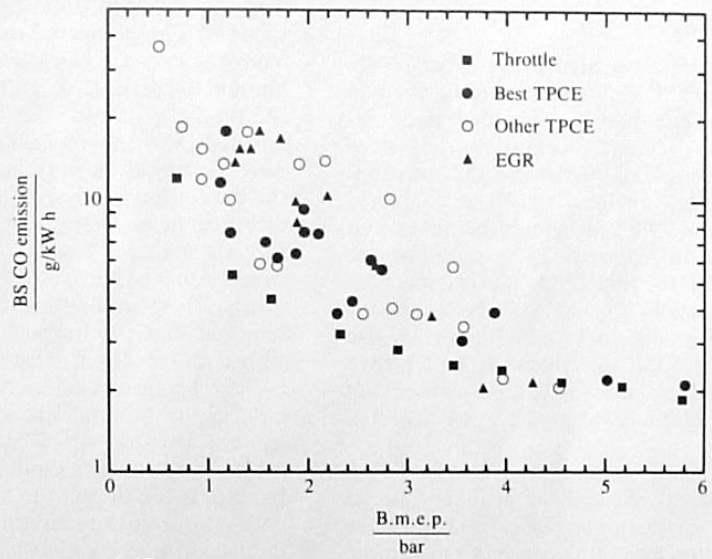
For vehicle applications, a rapid response to changing b.m.e.p. demand is required. Much of the dynamic performance of throttled engines is maintained in the TPCE system despite the presence of the heat exchanger and its unavoidable thermal lag time. This is achieved through the use of the diverter valve and the branched intake manifold. By this means cold, non-preheated

\* The minimum b.m.e.p. for the TPCE shown in Fig. 7 is smaller than that shown in Fig. 6 because the data in Fig. 7 were obtained in the Ford engine apparatus (see Section 3), which could provide higher  $T_{in}$  and thus lower b.m.e.p.

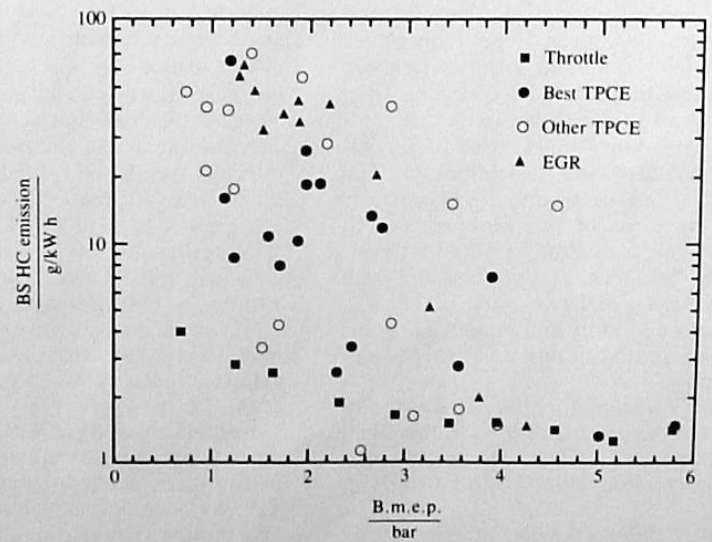




(a) Nitrogen oxides



(b) Carbon monoxide



(c) Unburned hydrocarbons

**Fig. 8** Comparison of brake specific exhaust emissions of NG-fuelled throttle-, TPCE- and EGR-controlled engines at 1200 r/min as a function of b.m.e.p.

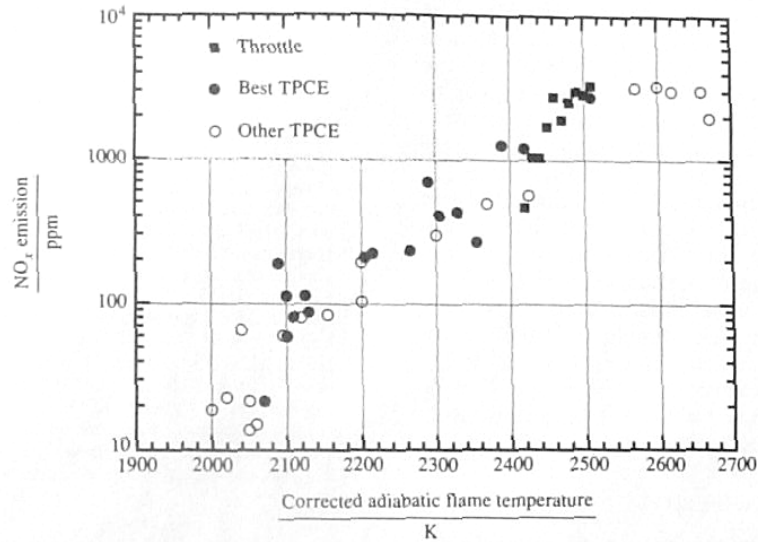


Fig. 9 Correlation of NO<sub>x</sub> emission at 1200 r/min to calculated adiabatic flame temperatures for NG-fuelled throttle- and TPCE-controlled engines

mixture is available without delay when the b.m.e.p. demand increases suddenly.

In most implementations to the TPCE concept, an auxiliary throttle would be useful under some conditions such as: (a) shortly after start-up, when the heat exchanger is cold and thus unable to provide sufficient preheating; (b) at very low b.m.e.p. demand, that is below the capabilities of the use of low  $\phi$  and high  $T_{in}$ ; (c) in vehicles when engine braking is desired, that is when coasting downhill; and (d) when a transient response faster than the capabilities of the baseline TPCE is required.

There are several favourable attributes of the TPCE concept that may aid in its possible implementation. Firstly, the TPCE has only one more moving part than

a conventional throttled engine, namely a diverter valve in the intake manifold. Thus, the TPCE system can be expected to have reliability similar to a conventional throttled engine. Also, it appears to be feasible to retrofit the TPCE system to existing gasoline or NG engines because only a change of the intake, exhaust and engine control systems is required for the basic installation. Of course, engines specifically designed for the TPCE application would realize more substantial performance gains. Furthermore, an advantage of the TPCE system for vehicles is that since throttling losses are eliminated at many operating conditions, there is little penalty (other than engine weight) for having the reserve power of a larger engine.

While the TPCE concept appears feasible in many

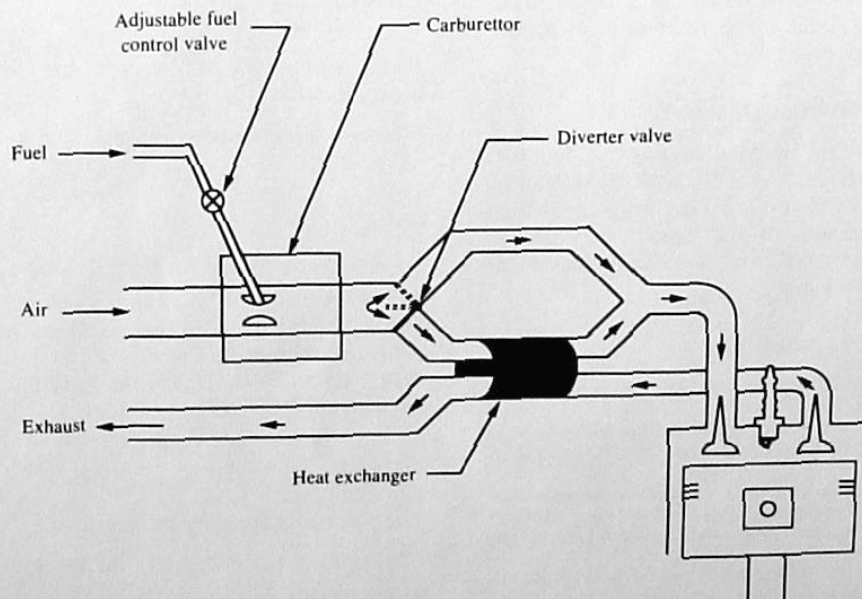


Fig. 10 Concept of a practical implementation of the TPCE system

respects, two issues have been identified that require further study before implementation. The first issue is the design of a heat exchanger which provides the necessary rate of heat transfer from the exhaust to intake streams, while having pressure drops that, for a given b.m.e.p., are small compared to the pressure losses that are associated with the use of throttling to provide the same b.m.e.p. Also, in vehicle applications, the size of the heat exchanger must be considered. The second issue is the definition of appropriate control strategies and control systems to implement these strategies. Four primary engine operating parameters need to be controlled: (a)  $\phi$ , (b)  $T_{in}$ , (c) ignition timing and (d) auxiliary throttle position (if installed). Since it is probably advantageous to operate near the LML, some form of lean-limit sensing, for example that described in reference (12), may be useful in this regard.

## 6 CONCLUSIONS

A concept for controlling the b.m.e.p. of a premixed-charge engine by varying equivalence ratio and intake temperature, rather than by throttling, was proposed, analysed and tested. It was found that at low b.m.e.p. the thermal efficiency of this engine was higher than that of throttled engines at the same b.m.e.p. due to the absence of throttling losses.  $NO_x$  emissions were much lower than throttled engines, CO emissions slightly higher and UHC emissions significantly higher. The main limitations on the performance of this engine were found to be due to the misfire and knock limits. The use of preheating provided improved lean-limit performance compared to unheated mixtures. While increased intake temperatures promoted knocking, the use of lean mixtures reduced the knocking tendency substantially. A variation of the concept, in which exhaust gas recirculation rather than intake charge preheating was employed, was found to have substantially inferior thermal efficiency and only modestly better  $NO_x$  performance. A discussion of the implementation of this throttleless engine concept indicates that two areas requiring further study are the exhaust-to-intake heat-exchanger design and the development of appropriate control systems.

## ACKNOWLEDGEMENTS

This work was supported by the Gas Research Institute under Grants 5088-260-1671 and 5088-260-1688, and by grants from the ARCO Foundation and the Mobil Foundation. The portion of the work performed at SwRI was supported by GRI and was conducted by Mr J. J. Cole and Dr S. R. King.

## REFERENCES

- 1 Heywood, J. B. *Internal combustion engine fundamentals*, 1989 (McGraw-Hill, New York).
- 2 Durbin, E. J. and Ronney, P. D. Method and apparatus for force or torque control of a combustion engine. US Pat. 5,184,592, 9 February 1993.
- 3 Karim, G. A. and Ali, I. A. Combustion, knock and emission characteristics of a natural gas fuelled spark ignition engine with particular reference to low intake temperature conditions. *Proc. Instn Mech. Engrs*, 1975, **189**, 139.
- 4 Karim, G. A. and Klat, S. R. The knock and autoignition characteristics of some gaseous fuels and their mixtures. *J. Inst. Fuel*, 1966, **39**, 118.
- 5 Ronney, P. D., Shoda, M., Waida, S. T., Westbrook, C. K. and Pitz, W. J. Knock characteristics of liquid and gaseous fuels in lean mixtures. *SAE Trans.*, 1992, **100**(4), 557; SAE paper 912311, 1991.
- 6 Lloyd, S. A. and Weinberg, F. J. A burner for mixtures of very low heat content. *Nature*, 1974, **251**, 47.
- 7 Lloyd, S. A. and Weinberg, F. J. Limits to energy release and utilisation from fuels. *Nature*, 1975, **257**, 367.
- 8 Hustad, J. E. and Sonju, O. K. Experimental studies of lower flammability limits of gases and mixtures of gases at elevated temperatures. *Combust. Flame*, 1988, **71**, 283.
- 9 Gaydon, A. G. and Wolfhard, H. G. *Flames: their structure, radiation and temperature*, 4th edition, 1979 (Chapman and Hall, London).
- 10 Quader, A. A. Lean combustion and the misfire limit in spark ignition engines. SAE paper 741055, 1974.
- 11 Ho, C. M. and Santaviceca, D. A. Turbulence effects on early flame kernel growth. SAE paper 872100, 1987.
- 12 Leshner, M. D., Stuart, Jr, J. W. and Leshner, E. Closed loop control for adaptive lean limit operation. SAE paper 780039, 1978.
- 13 Gluckstein, M. E. and Walcutt, C. End-gas pressure-temperature histories and their relation to knock. *SAE Trans.*, 1961, **63**, 529.

## APPENDIX 1

### Estimate of throttling losses

The goal of this analysis is to obtain a comparison of  $\eta_{th}$  for throttled and throttleless engines at the same b.m.e.p. The difference occurs because of the pumping work in the throttled engine. A relationship between the efficiencies is obtained by deriving an expression for the ratio of  $\dot{m}_f$  for the two engines at the same b.m.e.p. The throttled and throttleless engines will be designated by the subscripts 1 and 2 respectively. Also, the condition of WOT (that is  $P_{in} = P_{amb}$ ) along with  $T_{in} = T_{amb}$  and  $\phi = 1$  will be used as a reference state (designated by the subscript WOT). Note that all properties with the WOT subscript are the same for the throttled and throttleless engines.

Based on this discussion the following relations are evident:

$$b.m.e.p._1 = b.m.e.p._2 \equiv b.m.e.p. \quad (2)$$

$$\frac{\eta_{th,1}}{\eta_{th,2}} = \frac{\dot{m}_{f,2}}{\dot{m}_{f,1}} \quad (3)$$

The b.m.e.p. is the difference of the indicated work and the losses, that is

$$b.m.e.p._i = i.m.e.p._i - p.m.e.p._i - f.m.e.p. \quad \text{for } i = 1, 2 \quad (4)$$

and

$$b.m.e.p._{WOT} = i.m.e.p._{WOT} - p.m.e.p._{WOT} - f.m.e.p. \quad (5)$$

In equations (4) and (5), the f.m.e.p. is assumed constant and equal for the two engines. Also, assuming that the indicated thermal efficiency is constant, the i.m.e.p. is proportional to  $\dot{m}_f$ . Thus, the i.m.e.p. can be related to its value at WOT by

$$i.m.e.p. = i.m.e.p._{WOT} \left( \frac{\dot{m}_{f,i}}{\dot{m}_{f,WOT}} \right) \quad \text{for } i = 1, 2 \quad (6)$$

The p.m.e.p. is given by the relation

$$p.m.e.p._i = P_{ex} - P_{in,i} \quad \text{for } i = 1, 2 \quad (7)$$

where  $P_{ex}$  is assumed constant. For the throttleless engine,  $P_{in}$  is constant and assumed equal to  $P_{ex}$  (that is



there is a negligible pressure drop in the intake and exhaust systems); thus

$$P_{in,2} = P_{ex} \quad (8)$$

This is also true at WOT, that is

$$P_{in,WOT} = P_{ex} \quad (9)$$

Finally, for the throttled engine it is assumed that  $\phi$  and  $T_{in}$  are not varied. This has two consequences: firstly, the mass fraction of fuel in the intake mixture is constant and, secondly, the density of the intake mixture depends only on  $P_{in}$  and is linear with  $P_{in}$ . These facts imply that, for the throttled engine,  $\dot{m}_f$  is proportional to  $P_{in}$ , that is

$$\frac{\dot{m}_{f,1}}{\dot{m}_{f,WOT}} = \frac{P_{in,1}}{P_{in,WOT}} \quad (10)$$

The twelve relations (2) to (10) can be combined to obtain an expression for the ratio of thermal efficiencies as a function of b.m.e.p./b.m.e.p.<sub>WOT</sub>:

$$\frac{\eta_{th,1}}{\eta_{th,2}} = \left( 1 + \frac{P_{ex}}{i.m.e.p._{WOT}} \right) \times \left\{ 1 - \frac{P_{ex}}{(b.m.e.p./b.m.e.p._{WOT})(i.m.e.p._{WOT} - f.m.e.p.) + P_{ex} + f.m.e.p.} \right\} \quad (11)$$

Equation (11) is plotted in Fig. 11 for parameters that are representative of the experimental conditions, namely  $P_{ex} = 1$  atm,  $i.m.e.p._{WOT} = 6.46$  bar and  $f.m.e.p. = 0.68$  bar ( $i.m.e.p._{WOT}$  was estimated from the sum of the measured  $b.m.e.p._{WOT}$  and  $f.m.e.p.$ ). Also shown for comparison are the results for an idealized engine with  $f.m.e.p. = 0$ . Figure 11 shows that, as expected,  $\eta_{th}$  is the same for the two engines at WOT but as b.m.e.p. decreases,  $\eta_{th}$  is lower for the throttled engine. For the case  $f.m.e.p. = 0.68$  bar, as b.m.e.p. approaches zero,  $\eta_{th}$  for the throttled engine is about

half that of the throttleless engine. This indicates that in the throttled engine near idle, roughly half the fuel is used to overcome mechanical friction and half is used to overcome pumping losses. In the limit  $f.m.e.p. = 0$ , the throttleless engine requires no fuel at idle. Figure 11 also shows that at a typical vehicle operating condition of  $b.m.e.p./b.m.e.p._{WOT} = 30$  per cent,  $\eta_{th}$  would improve by 19 per cent if throttling losses could be eliminated.

## APPENDIX 2

### Estimate of TPCE operating map

The goal of this analysis is to obtain a semi-quantitative estimate of the b.m.e.p. and operating limits (of  $\phi$  and  $T_{in}$ ) of the TPCE. Consequently, some of the assumptions made are clearly not adequate for quantitative performance predictions, but may suffice to show qualitative trends.

As discussed in Section 1, TPCE operating limits are set by the following restrictions: (a)  $\phi < 1$ , (b)  $T_{in} > T_{amb}$ , (c) combinations of  $\phi$  and  $T_{in}$  that are smaller than the knock-limited values and (d) combinations of  $\phi$  and  $T_{in}$  that are larger than their values at the LML. As a rough estimate, it is presumed that the knock limit is defined by a constant  $T_{eg}$ , independent of the end-gas pressure. This type of behaviour was observed by Gluckstein and Walcutt (13), though they studied only near-stoichiometric mixtures. It is also assumed that the LML is defined by a constant  $T_{ad}$ , which is justified in Section 4.1. To simplify the analysis, an ideal-gas cycle with constant specific heats and gas constant, an adiabatic and isobaric intake process, isentropic compression and expansion, and constant-volume combustion at the minimum cylinder volume are assumed. The post-compression, post-combustion and post-expansion states are designated 2, 3 and 4 respectively.

First consider the estimate of the final end-gas temperature, that is of the last parcel of end-gas to burn. This gas has been compressed isentropically from pressure  $P_{in}$  to  $P_3$ , starting from temperature  $T_{in}$ ; hence its

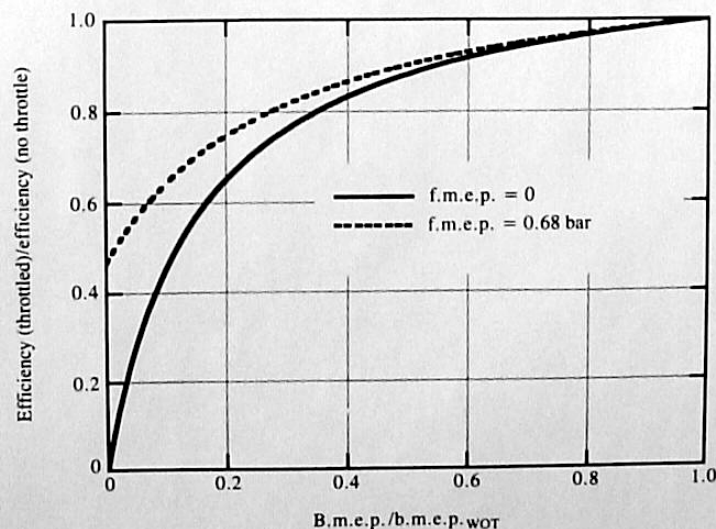


Fig. 11 Predicted [see equation (11)] ratio of brake thermal efficiencies of throttled and throttleless engines with  $i.m.e.p._{WOT} = 6.46$  bar,  $P_{ex} = 1.00$  bar and  $f.m.e.p. = 0$  or  $0.68$  bar

temperature is

$$T_{eg} = T_{in} \left( \frac{P_3}{P_{in}} \right)^{(\gamma-1)/\gamma} \quad (12)$$

To determine  $P_3$ , note that at the end of the (isentropic) compression process

$$P_2 = P_{in} r^\gamma \quad (13)$$

$$T_2 = T_{in} r^{\gamma-1} \quad (14)$$

and at the end of the (constant-volume) combustion process

$$T_3 = T_2 + \Delta T_c \phi \quad (15)$$

In equation (15), the temperature rise due to combustion ( $\Delta T_c \phi$ ) is assumed to be proportional to  $\phi$  since the fuel mass fraction is almost linear with  $\phi$ . Note that  $\Delta T_c$  is the *constant-volume, stoichiometric* value. Using the ideal-gas law for constant volume,

$$\frac{P_3}{P_2} = \frac{T_3}{T_2} \quad (16)$$

Combining equations (12) to (16) yields

$$T_{eg} = T_{in} r^{\gamma-1} \left( 1 + \frac{\Delta T_c \phi}{T_{in} r^{\gamma-1}} \right)^{(\gamma-1)/\gamma} \quad (17)$$

To determine the LML, an estimate of  $T_{ad}$  (that is the temperature of the first parcel of gas to burn) is required. Since the ratio of the temperature rise for constant-volume and constant-pressure combustion is  $\gamma$ ,

$$T_{ad} = T_2 + \frac{\Delta T_c \phi}{\gamma} = T_{in} r^{\gamma-1} + \frac{\Delta T_c \phi}{\gamma} \quad (18)$$

By assumption, equations (17) and (18) for constant  $T_{eg}$  and  $T_{ad}$  define the knock and lean misfire limit

curves respectively. Rather than specifying these temperatures *a priori*, these curves are 'anchored' at one point in the  $\phi$ - $T_{in}$  plane by consulting existing experimental data. A typical knock limit for NG at  $\phi = 1$  (extrapolated to  $r = 8$ ) is  $T_{in} = 510$  K (4). A typical value of the LML for many hydrocarbon fuels is  $\phi = 0.7$  at  $T_{in} = 300$  K (1, 3). For the representative values  $\Delta T_c = 2250$  K,  $\gamma = 1.3$  and  $T_{amb} = 300$  K, these data correspond to  $T_{ad} = 1770$  K and  $T_{eg} = 1260$  K. Figure 1 shows the predicted knock and misfire limit curves obtained using these values.

The i.m.e.p. is estimated by assuming a constant indicated thermal efficiency (as in Appendix 1), so that the i.m.e.p. is proportional to the mass of fuel burned. The mass of fuel is proportional to  $\phi$  and to  $\rho_{eyl}$ . In the TPCE, only  $T_{in}$  affects  $\rho_{eyl}$  (that is  $P_{in}$  is constant); hence

$$\frac{\text{i.m.e.p.}}{\text{i.m.e.p.}_{\text{WOT}}} = \left( \frac{T_{in}}{T_{amb}} \right) \phi \quad (19)$$

Lines corresponding to  $\text{i.m.e.p.}/\text{i.m.e.p.}_{\text{WOT}} = 0.75, 0.5$  and  $0.25$  are shown in Fig. 1. Note that the temperature after expansion is given by

$$T_4 = \frac{T_3}{r^{\gamma-1}} \quad (20)$$

which, when combined with equations (14) and (15), yields

$$T_4 = T_{in} + \frac{\Delta T_c \phi}{r^{\gamma-1}} > T_{in} \quad (21)$$

The fact that  $T_4 > T_{in}$  implies that the *ideal* exhaust temperature is high enough to preheat the fresh mixture to any desired  $T_{in}$ . Of course, in practice heat losses, materials limitations and knock limits will preclude very high  $T_{in}$ .